ResearchGate

See discussions, stats, and author profiles for this publication at: https://www.researchgate.net/publication/231237119

Hydrothermal Synthesis and Structure of Lead Titanate Pyrochlore Compounds

ARTICLE *in* CHEMISTRY OF MATERIALS · JULY 2003

Impact Factor: 8.35 · DOI: 10.1021/cm0301468

CITATIONS
18

READS
11

10 AUTHORS, INCLUDING:

Jing Ju
Peking University
36 PUBLICATIONS **359** CITATIONS
SEE PROFILE

Dejun Wang
Dalian University of Technology
44 PUBLICATIONS **133** CITATIONS
SEE PROFILE

Guobao Li
Peking University
127 PUBLICATIONS **1,253** CITATIONS
SEE PROFILE

Available from: Dejun Wang
Retrieved on: 02 February 2016

Hydrothermal Synthesis and Structure of Lead Titanate Pyrochlore Compounds

Jing Ju,[†] Dejun Wang,[†] Jianhua Lin,*[,†] Guobao Li,[†] Jing Chen,[‡] Liping You,[‡] Fuhui Liao,[†] Nianzu Wu,[§] Huizhong Huang,[§] and Guangqing Yao[†]

The State Key Laboratory for Rare Earth Materials Chemistry and Applications, College of Chemistry and Molecular Engineering, Electron Microscopy Laboratory, College of Physics, and The State Key Laboratory of Molecular Dynamic and Stable Structures, College of Chemistry and Molecular Engineering, Peking University, Beijing 100871, People's Republic of China

Received January 13, 2003. Revised Manuscript Received May 29, 2003

Systemic syntheses showed that the lead titanate pyrochlore phases formed under hydrothermal reactions in a certain range of KOH concentrations. The obtained pyrochlore phases all crystallize in the cubic structure. In comparison with typical pyrochlore structure, the O′ site in $Pb_2Ti_2O_6O'$ is vacant. In addition, considerable Pb vacancies are present in the samples obtained with high KOH content. Pb(IV) is present in these samples as confirmed by structural and spectroscopic studies. The distribution of metal atoms (Pb and Ti) in pyrochlore phases depends crucially on the KOH content in the starting materials. Higher KOH content tends to form ordered structures where Ti and Pb occupy 16c and 16d positions, respectively. While in the lower KOH content samples, Ti and Pb tend to be randomly distributed within these two sites. The morphology of the pyrochlore samples obtained by hydrothermal synthesis is uniformed spherical aggregates, which are formed by sparsely jointed nanoparticles. Thus, these materials contain narrowly distributed cavities and exhibit rather high surface area. The lead titanate pyrochlore is not stable at high temperature and transforms to the perovskite phase above 651 °C.

Introduction

Lead titanate perovskite is a typical displacive ferroelectric material. The large ionic shift leads to a particularly large room-temperature spontaneous polarization, which is in fact among the largest in the perovskite family.[1,2] In addition, the lead titanate perovskite also shows high Curie temperature, high pyroelectric coefficient, and low dielectric constant, and those properties render the lead titanate perovskite an attractive ferroelectric material for pyroelectric, electrooptical, and nonlinear optical material applications. Recently, considerable attention has been focused on growth of thin films of lead titanate perovskite by various methods, such as chemical vapor deposition and sol−gel processes. However, a second phase, which was assigned to be lead titanate pyrochlore, was often present in the perovskite thin films ($PbTiO_3$ or Pb$(Zr,Ti)O_3$).[3] The presence of this impurity phase in the films significantly reduces the relative permittivity of the ferroelectric films of the lead perovskite and, thus, it should be avoided in the film process.[4]

Pyrochlore is a well-known structural family that includes a large number of compounds with a general formula of $A_2B_2X_6X'$, in which A and B are metal atoms and X and X′ are anions at different crystallographic sites.[5,6] In the pyrochlore structure, the *B* atoms are octahedrally coordinated; thus, the B_2X_6 forms a diamond-like octahedral framework. While the A_2X' also forms a diamond-net that is interpenetrating with the B_2X_6 octahedral framework. Figure 1 showed the structure of pyrochlore, where to emphasize the octahedral framework the X′ atoms were omitted. Alternatively, the structure of pyrochlore can also be derived from the fluorite structure, from which one-eighth of the anions are removed systematically so as to confer near-octahedral coordination around B atoms and, meanwhile, to retain the cubic coordination of A atoms as in the fluorite. The metal atoms (A + B) in the pyrochlore structure in fact maintain fcc, like that in the fluorite, but they are ordered in two different sites (16d and 16c). Furthermore, the B_2X_6 octahedral framework is the rigid part in the structure, so in the same cases the pyrochlore structures are present with vacant A or X′ positions.

* Corresponding author. E-mail: jhlin@chem.pku.edu.cn. Telephone: +86 10 62751715, Fax: +86 10 62751708.

[†] The State Key Laboratory for Rare Earth Materials Chemistry and Applications, College of Chemistry and Molecular Engineering.

[‡] Electron Microscopy Laboratory, College of Physics.

[§] The State Key Laboratory of Molecular Dynamic and Stable Structures, College of Chemistry and Molecular Engineering.

(1) Lines, M. E.; Glass, A. M. *Principles and Applications of Ferroelectrics and Related Materials*; Oxford University Press: Oxford, 1977.

(2) Jaffe, B.; Cook, W. R., Jr.; Jaffe, H. *Piezoelectric Ceramics*; Academic Press: New York, 1971.

(3) Krupanidhi, S. B.; Hu, H.; Kumar, V. *J. Appl. Phys.* **1992**, *71*, 376.

(4) Klee, M.; Eusemann, R.; Waser, R.; Brand, W.; van Hal, H. *J. Appl. Phys.* **1992**, *72*, 1566.

(5) Wells, A. F. *Structural Inorganic Chemistry*; Oxford University Press: Oxford, 1984.

(6) Ramesha, K.; Sebastian, L.; Eichhorn, B.; Gopalakrishnan, J. *Chem. Mater.* **2003**, *15*, 668.

10.1021/cm0301468 CCC: $25.00 © 2003 American Chemical Society
Published on Web 07/26/2003

Table 1. Reaction Conditions and Products of Lead Titanate by Hydrothermal Method

sample no.	Pb/Ti	KOH (mol·dm^{-3})	temp (°C)	time (h)	products[a]	Pb/Ti in products EDX	XPS	ICP	weight loss[b] (%)	surface area (m^2/g)
S-1	1	0	180	24	TiO_2					
S-2	1.5	0.05	180	48	Py	0.98		1.01	0	21.8
S-3	1.5	0.1	180	48	py	0.93	0.90	0.98	0.46	28.9
S-4	1.5	0.25	180	48	Py	0.81	0.83	0.83	1.37	54.6
S-5	1.5	0.50	180	24	Py	0.75	0.75	0.86	1.38	70.8
S-6	1.5	0.60	180	24	PY+ trace PE					
S-7	1.5	0.75	180	48	trace PY + PE					
S-8	1.5	1.00	180	48	Pe					
S-9	1.5	2.00	180	48	Pe					2.4
S-10	1.5	3.00	180	48	Pe					1.8

[a] PY, pyrochlor-type lead titanate; PE, perovskite-type lead titanate. [b] The weight loss was determined by thermogravimetry at about 651 °C.

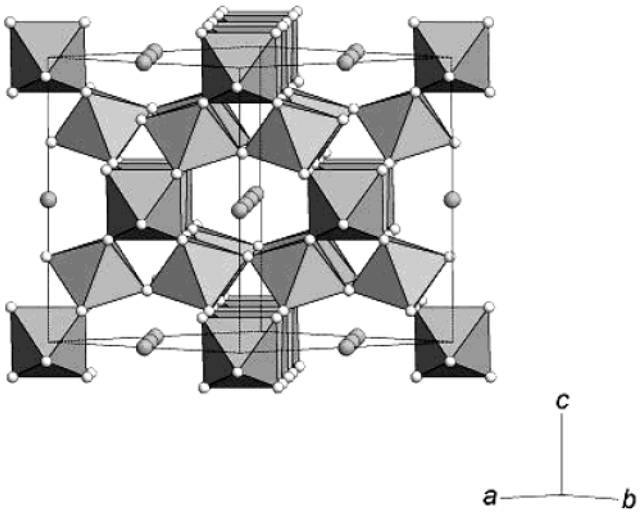

Figure 1. Structure of pyrochlore-type. The diamond-like octahedral framework of B_2X_6 is emphasized. The large balls are the A atoms and the X′ atoms are omitted in the figure.

It was reported many years ago[7] that lead titanate pyrochlore $Pb_2Ti_2O_{6+x}$ could be precipitated during the process of devitrification of lead glasses containing 10−20% TiO_2. Very recently, pyrochlore thin film[8] was obtained by pulsed laser deposition on the (100) CeO_2 substrate. The stoichiometry of the film is significantly deviated from that proposed previously. Similar results were obtained for perovskite thin films obtained by other techniques.[9−11] In addition, lead titanate pyrochlore was also observed as an impurity phase during the hydrothermal synthesis of lead titanate perovskite $PbTiO_3$.[12−16] As a mater of fact, an unknown phase observed by Cheng et al.[17] during their hydrothermal study on the PbO−TiO_2 system may also relate to the pyrochlore structure. But the composition they declared was lead-rich instead of deficient. Nevertheless, thus far the single-phase bulk sample of the lead titanate pyrochlore has not yet been obtained, probably because of its close stoichiometry to perovskite, as well as its metastable nature at high temperature. In this paper, we report synthesis of single-phase bulk samples of lead titanate pyrochlore by using hydrothermal reaction. As we shall show below, the formation and the structure of lead titanate pyrochlore depend strongly on the KOH content in the reaction systems, and moreover, Pb vacancies and random substitution of the metals atoms are present in these phases.

Experimental Section

Synthesis. All reagents are commercially available and were used without further purification. Lead acetate ($Pb(Ac)_2$·$3H_2O$) and titanium butoxide (tetra-*n*-butyl titanate, Ti-$[O(CH_2)_3CH_3]_4$, were used as the starting materials. $Pb(Ac)_2$ aqueous solution and $Ti[O(CH_2)_3CH_3]_4$ ethanol solution were added to a KOH aqueous solution with a ratio of Pb/Ti = 1.5. The acidity of the system is crucial for the product, so the experiments with different KOH contents were conducted as shown in Table 1. The reaction systems were first heated under stirring until the total volume of the feedstock was about 75 mL, which was then charged into a 100-mL Teflon-lined stainless steel autoclave apparatus. The hydrothermal reactions were conducted at 180 °C for 1−2 days. After the autoclave apparatus was cooled to room temperature, the products were filtered and washed with deionized water until neutrality is reached.

Characterization. Powder X-ray diffraction data were recorded on a Rigaku D/Max-2000 diffractometer at 50 kV and 100 mA for Cu Kα radiation. TG-DTA measurements were carried out with a Thermal Analyst 2100 System (Du Pont Instruments) with a heating rate of 10 °C min^{-1} in air. The electron diffraction was measured with a Hitachi-9000 transmission electron microscope and the morphology was done on a JEM-200 CX TEM and an AMRAY 1910 FE SEM. The adsorption and desorption isotherms were measured with a Micromerities ASAP2010 v3.02. Before the measurements, the samples were activated at 200 °C under vacuum for 4 h. Chemical analysis was conducted by standard EDX on Hitachi-9000 and by the ICP method. The oxidation state of lead cations was studied by photoelectron spectroscopy (XPS) (Axis Ultra, Shimadgu-Kratos) at 15 kV and 15 mA using an Al Kα monochromator. The step was 1 eV for the primary survey scan and was 0.1 eV for the narrow scan. The IR spectra were carried out on a Nicolet Magna-IR-750 series II. The content of carbon was measured with Elementar Vario EL. ac impedance of the samples pasted with Pt was measured with a HP4192A impedance analyzer in the frequency range from 1 kHz to 12 MHz between 200 and 800 °C. For structure refinement, the powder X-ray diffraction data were collected with a Bruker D8 diffractometer at 40 kV and 50 mA for Cu

(7) Martin, F. W. *Phys. Chem. Glasses* **1965**, *6*, 143.
(8) Hamedi, L'H.; Guilloux-Viry, M.; Perrin, A.; Li, Z. Z.; Raffy, H. *J. Solid State Chem.* **2001**, *158*, 40.
(9) Lee, J.; Safari, A.; Pfeffer, R. L. *Appl. Phys. Lett.* **1992**, *61*, 1643.
(10) Tabata, H.; Kawai, T.; Kawai, S.; Murata, O.; Fujioka, J.; Minakata, S. *Appl. Phys. Lett.* **1991**, *59*, 2354.
(11) Chen, S. Y.; Chen, I. W. *J. Am. Ceram. Soc.* **1994**, *77*, 2337.
(12) Moon, J.; Li, T.; Randall, C. A.; Adair, J. H. *J. Mater. Res.* **1997**, *12*, 189.
(13) Suzuki, M.; Uedaira, S.; Masuya, H.; Tamura, H. *Ceramics Transactions*, Vol. 1, Ceramic Powder Science II; The American Ceramic Society Inc.: Westerville, OH, 1988; p 163.
(14) Cheng, H.; Ma, J.; Zhao, Z.; Qiang, D. *Am. Ceram. Soc.* **1992**, *75*, 1125.
(15) Cheng, H.; Ma, J.; Zhao, Z.; Zhang, H.; Qiang, D.; Li, Y.; Yao, X. *Proceedings of C-MRS International' 9*; Elsevier: Amsterdam, 1990; Vol. II, pp 509−140.
(16) lencka, M. M.; Riman, R. E. *J. Am. Ceram. Soc.* **1993**, *76*, 2649.
(17) Cheng, H.; Ma, J.; Zhao, Z. *Chem. Mater.* **1994**, *6*, 1033.

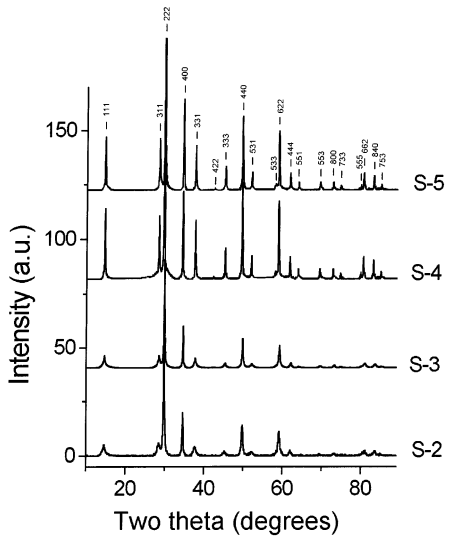

Figure 2. Powder X-ray diffraction patterns of lead titanate pyrochlore phases obtained in 0.05 mol·dm^{-3} (S-2), 0.1 mol·dm^{-3} (S-3), 0.25 mol·dm^{-3} (S-4), and 0.5 mol·dm^{-3} (S-5) KOH systems. The indices of the individual reflections are indicated for S-5.

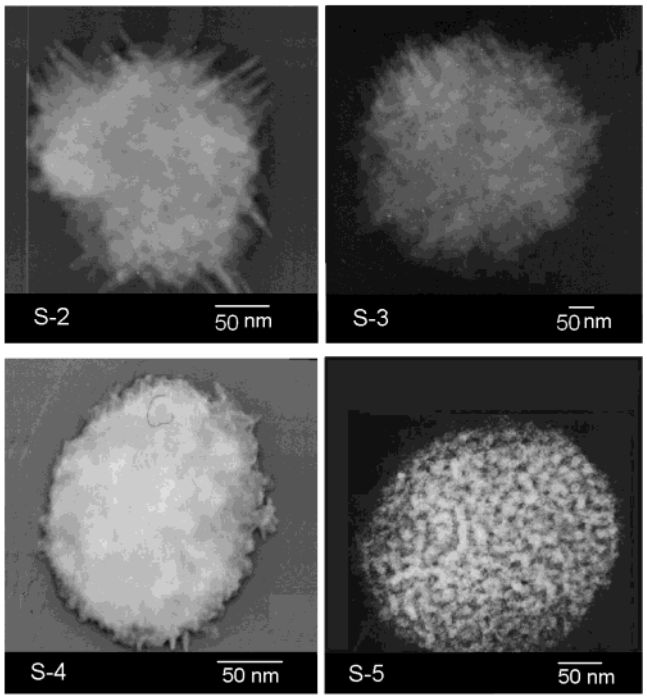

Figure 3. Transmission electron micrographs of lead titanate pyrochlore phases obtained in 0.05 mol·dm^{-3} (S-2), 0.1 mol·dm^{-3} (S-3), 0.25 mol·dm^{-3} (S-4), and 0.5 mol·dm^{-3} (S-5) KOH systems.

$K\alpha_1$ ($\lambda = 1.54056$ Å) radiation. The Rietveld refinement of lead titanate pyrochlore sample was carried out using GSAS with all isotropic displacive parameters.

Results and Discussion

Typical hydrothermal conditions for the synthesis of lead titanates are listed in Table 1. It can be seen that the products depend strongly on the KOH content in the loaded systems and other factors, such as reaction temperature and time, only have minor influence. On the basis of the products obtained, the reactions can be classified into three regions. The reaction without KOH yielded only TiO_2 as an insoluble product. With 0.05−0.5 mol·dm^{-3} KOH, single-phase products of lead titanate pyrochlore, which were golden in color, were obtained. When KOH content was beyond 1.0 mol·dm^{-3}, the products were single-phase perovskite $PbTiO_3$, which were light yellow in color. When the KOH content was between 0.5 and 1.0 mol·dm^{-3}, a mixture of pyrochlore and perovskite was produced. From this systematic study, different lead titanates phases can be purposively obtained by varying the KOH content in the systems.

Figure 2 shows the powder X-ray diffraction patterns (XRD) of the pyrochlore phases obtained with different KOH contents. Pyrochlore crystallizes in cubic structure[18] with the space group of *Fd*3*m* (No. 227). The powder X-ray diffraction and electron diffraction patterns (electron diffraction patterns of S-3 and S-5 are included in the Supporting Information) of lead titanate pyrochlore phases can be readily indexed with the cubic cell. In Figure 2 the indices of the individual reflections are also included, where one can see that, although the diffraction patterns are similar, relative intensities and broadening of reflections are different from one to another. For the samples obtained with high KOH content (S-4 and S-5), the reflections are sharp and intense with rather homogeneous bandwidth. For the low KOH content samples (S-2 and S-3), the diffraction patterns are still pyrochlore-type, but several reflections become broad and weak. An obvious trend is that the lower the KOH content, the weaker and broader these reflections are. Inspection of the diffraction patterns revealed that the broad reflections all have odd *h*,*k*,*l* indices. This means that a certain structure distortion is present in these phases and, the KOH content decreases, the distortion becomes more serious.

To understand the structure feature of these systems, the morphology of the samples was examined by TEM, as shown in Figure 3. All of the samples appear as spherical-shaped aggregates consisting of nanosized crystalline pyrochlore. The crystallites in the samples obtained with low KOH content (S-2 and S-3) are needle-shaped, while in that obtained with high KOH content, the crystallites are more regular with almost isotropic shape (S-5). It is well-known that the needle-shaped crystallites may introduce preferred orientation effect in the powder diffraction pattern. However, the broadening and the weakening of the odd *h*,*k*,*l* reflections in the low KOH content samples cannot be interpreted by any of those axial effects or distortions.

To learn the details of the structure, we carried out Rietveld refinement on the powder data of S-5. Figure 4 shows the profile fit of the XRD pattern. The structure refinement unambiguously shows that the X′ position (8b) is unoccupied in S-5 and the Ti (16c) and O (48f) positions are all fully occupied. According to the structural study of bismuth pyrochlore,[19−21] the A atoms may

(18) Subramanian, M. A.; Aravamudan, G.; Subba Rao, G. V. *Prog. Solid State Chem.* **1983**, *15*, 55.

(19) Radosavljevic, I.; Evans, J. S. O.; Sleight, A. W. *J. Solid State Chem.* **1998**, *136*, 63.

(20) Kahlenberg, V.; Bohm, H. *Cryst. Res. Technol.* **1995**, *30*, 237.

(21) Avdeev, M.; Haas, M. K.; Jorgensen, J. D.; Cava, R. J. *J. Solid State Chem.* **2002**, *169*, 24.

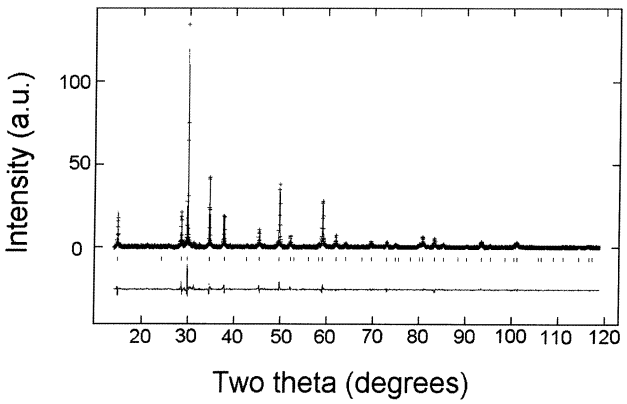

Figure 4. Profile fit of the powder X-ray diffraction pattern for S-5. The + represents the observed pattern and the solid line represents the calculated pattern. The reflection positions and difference curves are at the bottom of the figure.

Table 2. Refined Structural Parameters for Pyrochlore Lead Titanate Phase (S-5) at Room Temperature, Cubic Space Group *Fd*3*m* (No. 227), with Pb at 16d ($^1/_2$,$^1/_2$,$^1/_2$) (Model 1) or 96h (0,*y*,−*y*) (Model 2) Site, Ti at 16c (0,0,0), O at 48f (*x*,$^1/_8$,$^1/_8$)[a]

	model 1	model 2
a (Å)	10.36962(32)	10.37049(13)
y(Pb)	1/2	0.2397(16)
U_{iso}(Pb)	0.0304(9)	0.0226(26)
n(Pb@Pb)	1.37(2)	1.38(2)
U_{iso}(Ti)	0.0371(28)	0.0375(27)
n(Ti@Ti)	2	2
x(O)	0.3151(16)	0.3157(15)
U_{iso}(O)	0.056(8)	0.053(8)
goodness of fit	1.46	1.43
R_p (%)	10.0	9.9
R_{wp} (%)	13.1	13.0

[a] XRD data were collected on Bruker D8 with Cu Kα_1 radiation, 2θ range 14−120°, step 0.02°, 10 s/step. The structure refinement was carried out with GSAS.

deviate from the ideal (16d) position and distribute among the 96h positions. Two structure models were, therefore, used to refine the Pb positions, respectively, with the ideal Pb position (16d) and disordered position (96h), and the results are shown in Table 2. It can be seen that both models show similar agreement factors, but slight improvement was achieved for the disordered model (Model 2). Nevertheless, both refinements revealed partial occupation at the Pb position, indicating that considerable Pb vacancies do exist in this material.

To further confirm the composition of the materials, chemical analyses were carried out with EDX, ICP, and XPS methods, and the results are listed in Table 1. It can be seen that the Pb/Ti ratio varies in different samples. In the low KOH samples, the Pb/Ti ratio is almost equal to 1. While in the high KOH content samples, Pb is definitely deficient, although the measured Pb/Ti shows somewhat different values using different methods. The deficiency of Pb in the materials could be compensated either by oxygen vacancies or by the presence of Pb(IV). It has been reported that bismuth titanate pyrochlore $Bi_{2-x}Ti_2O_{7-d}$[19−21] is also Bi-deficient. In this material Bi is in Bi(III) and the Bi vacancies are compensated by oxygen vacancies at the 8a site (X′). The oxygen atoms at the 48f site (X) are directly coordinated to the octahedral metal atoms; thus, it is unfavorable to have a large number of vacancies at this position. The presence of Pb(IV) in the pyrochlore

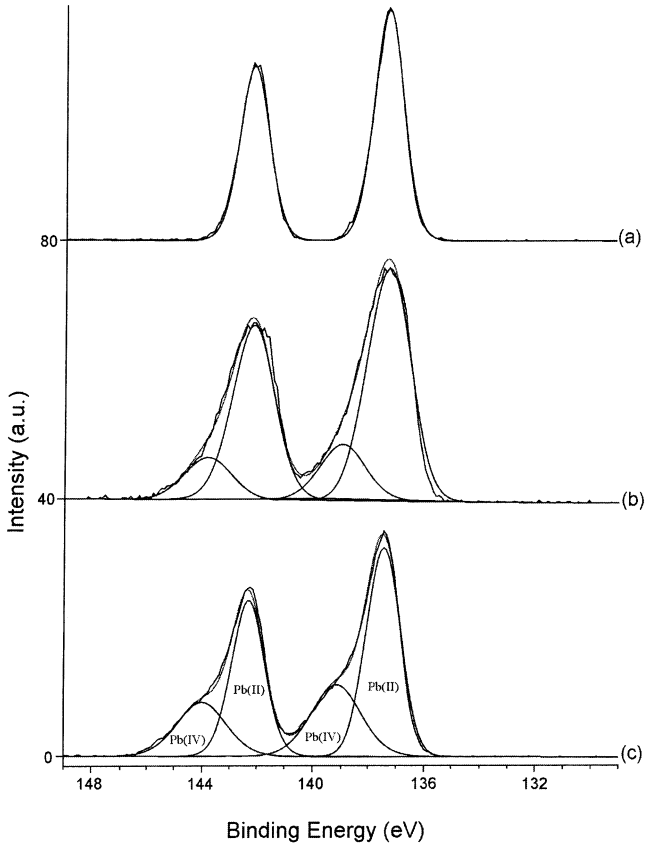

Figure 5. Photoelectron spectrum (XPS) of the lead titanate pyrochlore (a) S-3, (b) S-4, and (c) S-5. The contribution of Pb(II) and Pb(IV) was represented by curve fitting.

phase was also known in $Pb_2[B_{2-x}Pb_x]O_{7-y}$ (B = Ru and Ir).[22] However, the Pb(IV) in this material occupies the octahedral site (B site) and the A site is fully occupied by Pb(II). From structure refinement, we knew that the Ti (16c) and O (48f) positions are likely fully occupied in the S-5 sample; thus, the possible compensation in this material might be Pb(IV) at the A site. Figure 5 shows X-ray photoelectron spectroscopic (XPS) spectra of S-3, S-4, and S-5. The peaks at 137.5 and 142.36 eV correspond to the $4f_{7/2}$ and $4f_{5/2}$ of Pb(II) and those at 139.18 and 144.04 eV correspond to the $4f_{7/2}$ and $4f_{5/2}$ of Pb(IV). It can be seen that both S-4 and S-5 contain Pb(IV), while in S-3 the content of Pb(IV) is too low to be detected by XPS. From XPS spectra one can estimate the Pb(II)/Pb(IV) ratio, which is about 3.83 and 1.97 for S-4 and S-5, respectively. These observations are in accordance with the Pb/Ti ratio obtained by chemical analyses shown in Table 1.

The presence of Pb(IV) in these materials is supported by thermal analysis. Figure 6 shows typical DTA and TGA curves for S-5. The as-synthesized sample contains considerable adsorbed water and organic residues, as indicated by IR spectra in Figure 7, where absorption bands at 2926, 1344, 1545, and 1413 cm^{-1} originate from, respectively, νas(CH), δs(CH_3), ν(C=O), and ν(C−O) of acetic acid[23] and that at 3400 cm^{-1} originates from water molecules. The material loses about 4.2 wt % weight gradually up to 280 °C and then a sharp weight

(22) Horowitz, H. S.; Longo, J. M.; Lewandowski, J. T. *Mater. Res. Bull.* **1981**, *16*, 489.
(23) Roziere, J.; Potier, J. *J. Inorg. Nucl. Chem.* **1973**, *35*, 1179.

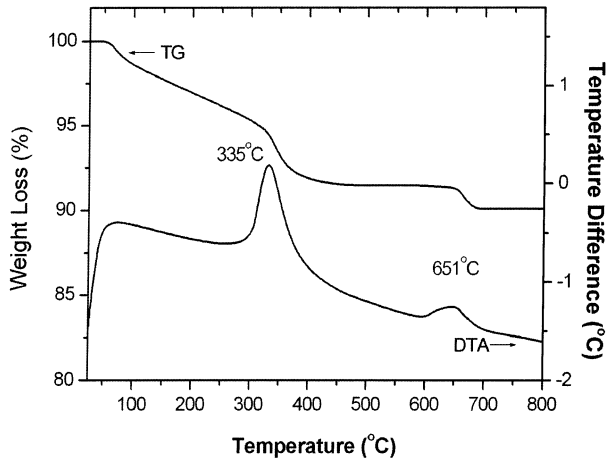

Figure 6. TGA and DTA curves for an as-synthesized sample S-5.

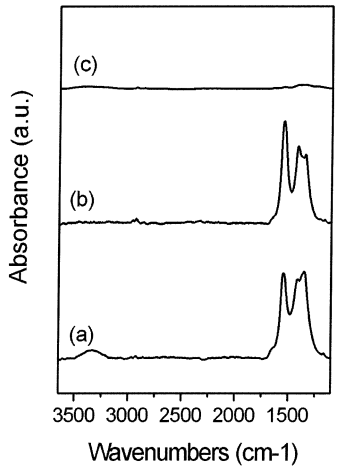

Figure 7. IR spectra of the S-5 samples (a) as-synthesized and calcinated at (b) 180 °C and (c) 450 °C, respectively.

loss (about 4.1 wt %) around 335 °C occurs together with an exothermal DTA peak. As shown in Figure 7, the water molecules were completely removed at about 180 °C and IR peaks of acetic acid disappear after the heating treatment at 450 °C.[24] Thus, the weight losses below 400 °C are caused by the removal of water molecules and organic residues. At about 651 °C additional small weight loss (about 1.38 wt %) accompanied by an exothermal effect was observed. This can be attributed to reduction of Pb(IV) to Pb(II) and removal of oxygen from the pyrochlore phase (calculated 1.59 wt % if fully reduced from $Pb_{1.5}Ti_2O_6$). It is also worth noticing a substantial correlation between the weight loss at 651 °C and the Pb/Ti ratio in the materials (Table 1), which shows that the samples prepared with low KOH content contain both less Pb vacancies and less Pb(IV). The dependence of Pb(IV) on the KOH content in the starting materials can easily be understood by considering the relative stability of Pb(IV) and Pb(II) in the reaction systems. As is well-known, the electrode potential of Pb(IV) ↔ Pb(II) depends strongly on the pH

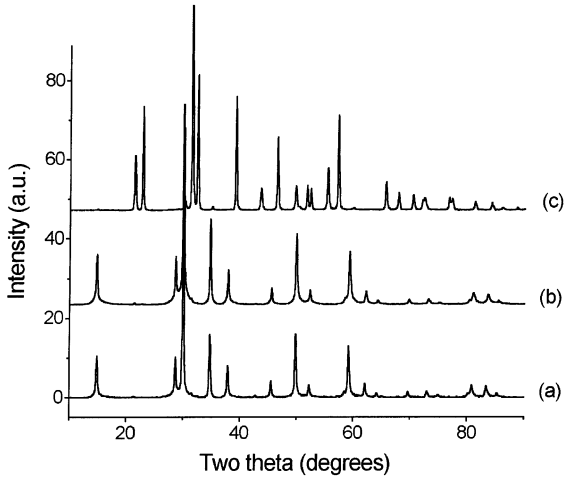

Figure 8. Powder X-ray diffraction pattern of the S-5 sample after heating treatment at (a) 180 °C, (b) 450 °C, and (c) 680 °C, respectively.

value of the system. Under strong basic conditions, the Pb(IV) becomes fairly stable; therefore, the pyrochlore samples obtained with high KOH content (S-5) contains more Pb(IV) and vice versa.

Figure 8 shows XRD patterns of the S-5 sample after calcination at 180, 450, and 680 °C, respectively. The pyrochlore structure retains at 180 and 450 °C and transforms to the perovskite at 680 °C. The phase transition from pyrochlore to perovskite seems to correlate with the reduction of Pb(IV), as indicated by DTA and TGA measurement. Furthermore, the spherical aggregation morphology of the sample was retained after the heating treatment at 450 °C (Figure 9b). However, at 680 °C the morphology of the sample became cubic crystallites when perovskite phase was formed (Figure 9c). Interestingly, the pyrochlore phases of such spherical morphology obtained by hydrothermal synthesis exhibits typical mesoporous adsorption behavior, as shown in Figure 10. This unusual property originates from the cavities between the jointed nanoparticles. The cavities in the aggregates are uniformly distributed at about 3−4 nm, as shown in the insert of the figure. Table 1 lists the BET surface area of these samples. One can see that S-5 has the largest surface area of about 70.8 m^2/g among these samples. The water and organic molecules were adsorbed in the cavities in the as-synthesized samples and are removed in a stepwise manner during heating treatment. It is known that some of the pyrochlore phases are semiconductors with non-Arrhenius behavior.[6,25] The mesoporous morphology of such oxides may have potential applications in photocatalysis, optics, and electronics.[26] However, it is difficult to measure the conductivity of the lead titanate pyrochlore obtained by hydrothermal synthesis because of its metastable nature. The lead titanate perovskite phase obtained by heating pyrochlore at 680 °C, however, is a typical dielectric material with conductivity of about 10^{-7} $\Omega^{-1}\cdot cm^{-1}$ at 340 °C.

Finally, we move to the structure feature of the samples synthesized with low KOH content (S-2 and

(24) The elemental analysis of the S-5 sample after being heated at 180 °C indicates the presence of carbon (about 1.81 wt %), which corresponds to 4.5 wt % HAc in the material. This value agrees reasonably well with the sharp weight loss around 335 °C on the TG curve. The carbon content decreases significantly after heating treatment at 450 °C (0.25 wt %).

(25) Ali, N.; Hill, M. P.; Labroo, S.; Greedan, J. E. *J. Solid State Chem.* **1989**, *83*, 178.
(26) Fchuth, F.; Schmidt, W. *Adv. Eng. Mater.* **2002**, *4*, 269.
(27) Lieckÿk, H. F. *Z. Anorg. Allg. Chem.* **1952**, *271*, 17.

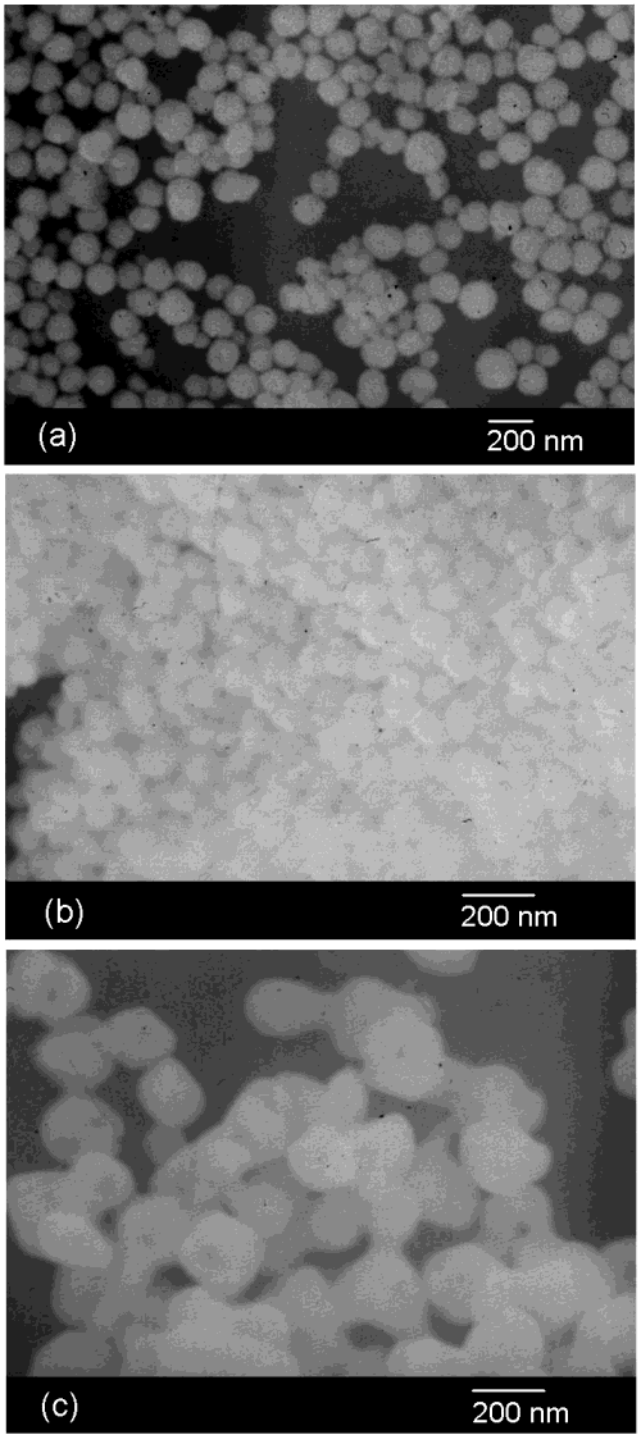

Figure 9. Scanning electron micrographs of S-5 sample (a) as-synthesized and calcinated at (b) 450 °C and (c) 680 °C, respectively.

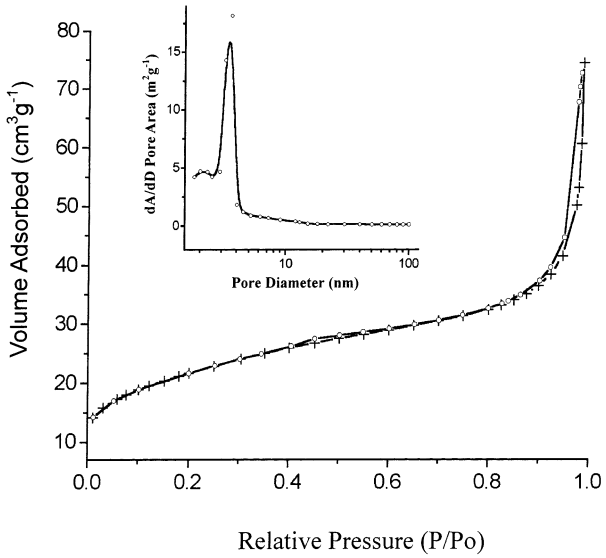

Figure 10. Nitrogen gas sorption isotherms for S-5 after calcination at 200 °C under vacuum (crosses, sorption; open circles, desorption). Inset, pore-size distribution plot from the desorption isotherm. The pore size was calculated by using the BJH method.

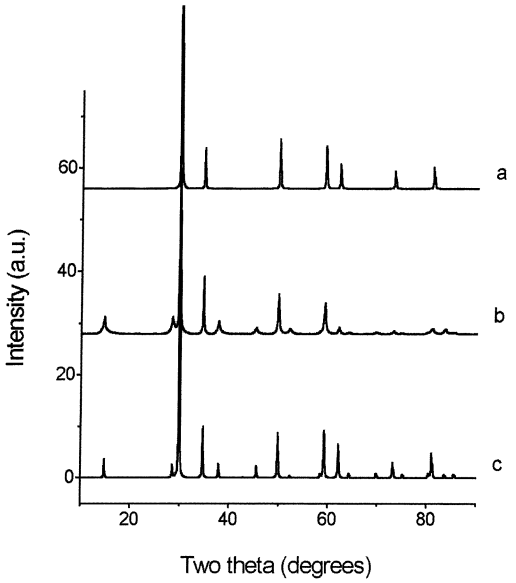

Figure 11. Powder X-ray diffraction patterns of lead titanates: (a) simulated pattern with fluorite-type structure,[27] (b) observed pattern for S-2, and (c) simulated pattern with pyrochlore-type structure [5] with 30% random substitution of the metal cations Pb and Ti in 16c and 16d sites.

S-3). As mentioned above, the XRD patterns of these pyrochlore phases feature in broadening and weakening of those reflections with the *h*,*k*,*l* of all odd numbers. Considering the structural relationship between pyrochlore and fluorite, the fully disordered structure may relate to the fluorite-type in which Ti and Pb are randomly distributed among the 16c and 16d sites. In Figure 11a we show a simulated powder pattern of the fluorite-type structure. It can be seen that the reflection peaks of the fluorite-type correspond very well to those sharp reflections in the observed S-2 powder pattern (Figure 11b). With exactly the same manner, one can simulate powder patterns with different randomness among the 16c and 16d positions and thus estimate the distribution of the metal atoms in the real structures. The powder pattern shown in Figure 11c was generated using 30% random substitution of Ti and Pb in 16c and 16d sites, which exhibits a similar intensity distribution as that observed for S-2, except the broadening.

In conclusion, we have studied the hydrothermal reactions of lead acetate and titanium butoxide in varied KOH systems and obtained various lead titanate phases with pyrochlore and perovskite structures. The pyrochlore phases can only be formed in moderate basic systems with $C_{KOH} \geq 0.05$ mol·dm^{-3} and the perovskite phases were obtained in strong basic systems $C_{KOH} \geq$

1.0 mol·dm^{-3}. The structural and spectroscopic studies revealed that the pyrochlore phase contains either considerable Pb(IV) and Pb vacancies or the metal atoms (Pb and Ti) are randomly distributed depending on the KOH content in the reaction systems. In addition, the lead titanate pyrochlore phases obtained with hydrothermal reactions feature in the spherical morphology of aggregates formed by sparsely jointed nanoparticles. The large surface area and the uniform distribution of the cavities may have potential applications in various fields, such as heterogeneous catalysis and electrocatalysis.

Acknowledgment. We are thankful for the financial support from NSFC and the State Key Basic Research Program.

Supporting Information Available: Tables of crystallographic data and related figures (PDF). This material is available free of charge via the Internet at http://pubs.acs.org.

CM0301468